

Enhancing the Mechanical Performance of Concrete Slabs through the Incorporation of Nano-sized Iron Oxide Particles (Fe_2O_3)

Non-local Bending Analysis

Amar Kecir¹, Mohammed Chatbi^{1*}, Zouaoui R. Harrat¹, Mohamed Bachir Bouiadjra^{1,2}, Mohammed Bouremana¹, Baghdad Krour¹

¹ Laboratoire des Structures et Matériaux Avancés dans le Génie Civil et Travaux Publics, University of Djillali Liabes, P. O. B. 89, Sidi Bel-Abbes 22000, Algeria

² Thematic Agency for Research in Science and Technology, ATRST, P. O. B. 62, El Harrach 16004, Algeria

* Corresponding author, e-mail: mohammed.chatbi@dl.univ-sba.dz

Received: 17 July 2023, Accepted: 12 February 2024, Published online: 18 April 2024

Abstract

The utilization of recycled iron in durable concrete production has gained attention for enhancing sustainability and resource efficiency. Simultaneously, incorporating nanoparticles as supplementary cementitious materials (SCMs) offers significant benefits. Introducing nano-sized iron particles (Fe_2O_3) into the cement paste results in a compact microstructure, improving strength, and durability. In this study, we investigate the bending behavior of concrete slabs reinforced with Fe_2O_3 nanoparticles using the non-local quasi-3D shear deformation theory based on Eringen's non-local differential constitutive relations. To characterize the elastic material properties of the nanocomposite, we employ Eshelby's homogenization model. In order to extend the applicability of our findings, we assume that the concrete plate rests on Kerr's foundation, which includes a shear layer connected to upper and lower springs. By deriving the equations of motion using the principle of virtual work, we establish a comprehensive framework for analyzing the bending of the concrete plate. To solve the equilibrium equations for a simply supported concrete plate, we present Navier's analytical solutions. Our investigation considers various influential parameters, such as the concentration of Fe_2O_3 nanoparticles in the concrete matrix, the elastic constants of the soil medium, different types of bending loads, and size-dependent nonlocal parameters. One of the most captivating findings of this study is that the incorporation of 30 wt% of iron nanoparticles in concrete leads to a remarkable improvement of 60% in the elastic properties of the material. Additionally, this same amount of iron nanoparticles has shown the potential to reduce the deflection of thin plates by over 60%.

Keywords

nano-composite concrete, Fe_2O_3 nanoparticles, bending analysis, Quasi-3D theory, Eringen's non-local theory, Kerr's elastic foundation

1 Introduction

In recent years, the application of various types of nano-reinforcements in concrete mixtures has emerged as a compelling topic, capturing the interest of numerous researchers and motivating them to develop advanced concrete with distinctive physical and chemical properties. Traditional materials like silica fume (Micro silica) and fly ash are being substituted with nano-sized components to fulfill specific mechanical requirements. Through the incorporation of carefully determined proportions of specific nanoparticles such as iron (Fe_2O_3), silica (SiO_2), titanium (TiO_2), nano-clays (NCs), and aluminum (Al_2O_3)

as reinforcements in a concrete matrix, the material's properties and performance can be enhanced in terms of strength, durability, and resistance to cracking, [1, 2].

For instance, Priyadarshana and Dissanayake [3] conducted an experimental investigation to compare the effect of nano-silica (nano- SiO_2), micro-silica (micro- SiO_2) and fly ash on the chemical resistance of concretes. They concluded that adding optimum proportions of combined nano and micro-silica can moderate the chemical resistance of the concrete, becoming therefore more resistant to the attacks of sulphatic environment. Furthermore,

additional research has addressed the mechanical and thermal implications of employing SiO_2 as reinforcements in concrete. In this respect, Mondal et al. [4], Rong et al. [5], Behzadian and Shahrajabian [6], Bidgoli and Saeidifar [7], have all deduced that adding nano- SiO_2 to concrete matrices resulted in improved compressive, tensile, flexural, and thermal resistance properties of the concrete. Besides, due to their nano scaled size in the range of 1–500 nm, nano-silica, have consequently produced shorter setting time and water permeability, allowing the concrete matrix to acquire a dense structure that leads to a strong resistance to chemical attacks. Therefore, nano-silica reinforcements can constitute parts of many concrete structures that we observe today. Recently, Harrat et al. [8] and Chatbi et al. [9] have investigated the analytical static behaviour of concrete beams and plates impregnated with silicon dioxide (SiO_2) nanoparticles by taking into account the agglomeration effect of nano-silica. Their studies revealed that incorporating SiO_2 nanoparticles in concrete leads to enhanced mechanical strength, resulting in reduced bending deflections. In the dynamic aspect, Jassas et al. [10] examined the forced vibration of concrete slabs reinforced with agglomerated SiO_2 nanoparticles using numerical methods. They employed the Mori-Tanaka model to determine the material properties of the nano-composite structure and account for agglomeration effects. Their findings indicate that increasing the volume percentage of SiO_2 nanoparticles up to 0.37 results in an increased linear frequency of the structure and a decreased maximum dynamic deflection. Furthermore, Rashmi and Padmapriya [11] have scrutinized the structural behaviour of a reinforced concrete beam that has been strengthened using nano silica of various proportions (1%, 2%, 3%, 4%, and 5%) along with other larger proportions of manufactured sand (25%, 40%, 50%, 75%, and 100%). In this respect, they figured out that the use of nano silica and manufactured sand in the beam specimen upsurge the flexural ultimate load, and eventually, enhance the flexural property of the concrete.

Other types of nanoparticles reinforcements are used in cement manufacturing, mortars and concrete mixtures. For instance, Nazari et al. [12] studied strength assessments and coefficient of water absorption of a high performance self-compacting concrete that contains different proportions of ZrO_2 nanoparticles. Likewise, Aly et al. [13] have launched a laboratory study of the properties of nano clay and waste-glass powder (NC/WGP) cement composites. The microstructure ASR, fracture energy,

compressive and flexural properties of cement mortars containing WGP as a cement replacement with and without NC were investigated and compared with a pure cement matrix. The results of their investigation showed that the incorporation of glass powder has a strengthening effect on the mechanical properties of cement mortars after 28 days of hydration. The results have also revealed that the mechanical properties of the cement mortars with a hybrid combination of glass powder and NC were all better than those of a plain mortar after 28 days of hydration. Moreover, the photo catalytic activities of TiO_2 dip-coated self-compacting glass mortars (SCGMs) in terms of air pollutant removal were investigated and compared by Guo et al. [14]. In addition, the weathering resistance of TiO_2 -coated cement mortars was evaluated. The results of their work suggest that the TiO_2 retained in the porosity of the dip-coated SCGM can still contribute to the elastic properties of the nano composite. Feng et al. [15] have tested the flexural strength of the prepared cement-based composites. Consequently, the flexural strength of the nano modified TiO_2 Portland cement paste reached the highest value with a dosage of 1.0 mass %. More importantly, the SEM observation shows that admixing the TiO_2 nano particles has largely decreased the quantity of internal micro cracks in the cement paste. By means of making many experiments, Joshaghani et al. [16] studied and compared the effects of different incorporated nanoparticles, namely nano- Al_2O_3 and nano- TiO_2 , on the performance of self-consolidating concrete (SCC) in terms of fresh, mechanical, and durability properties. Subsequently, the findings of their experiments demonstrated that the workability of the mixture have improved slightly with the addition of 3% only of nanoparticles, while increasing the value to 5% tend to minimize its workability. In fact, the incorporation of nanoparticles into the mixture tends to increase water demand as the nanoparticle content increases, resulting therefore in a reduced workability. Amoli et al. [17] investigated the nonlinear dynamic response of a concrete plate retrofitted with aluminum oxide (Al_2O_3) under both seismic load and magnetic field conditions. The study utilized analytical modeling employing Mori-Tanaka's model to determine the composite material properties while considering the agglomeration effect of Al_2O_3 nanoparticles. Their results indicated that with an increasing volume percentage of nanoparticles, the dynamic deflection decreases.

In particular, Ferric oxide (Fe_2O_3) is often used as a replacement of cement in a concrete matrix in order to increase the strength and reduce the shrinkage of the

concrete over time. This is because ferric oxide is able to form a dense nano structure within the concrete matrix, which helps to improve the strength and durability properties of the concrete. Hence, ferric oxide helps to improve the chemical resistance of the concrete and reduce permeability; making it more resistant to corrosion, Nazari et al. [18]. Experimentally speaking, it is worth noting that few researches have investigated the effect of ferric oxide (Fe_2O_3) on concrete properties. For example, Nazari et al. [19] dissected the effects of incorporating Fe_2O_3 nanoparticles on tensile and flexural strength of the concrete. On the other hand, Salemi et al. [20], have conducted various experiments to study the effect of iron nanoparticles on frost durability of concretes. Moreover, Nouri [21] investigated the stability of concrete pipes mixed with nanoparticles conveying fluid. Instead of cement, the Fe_2O_3 nanoparticles are rather used in the construction of the concrete pipes. In the prospect, it was concluded in light of those studies that the partial replacement of cement with nano phase Fe_2O_3 particles is likely to improve the split tensile and flexural strength of the concrete, but it tends to decrease its setting time. As far as analytical analyses of the concrete structures reinforced with iron nanoparticles are concerned, a wide range of knowledge gap was found in the literature despite the great attraction and the advantages that can be brought by modelling nano-composites regarding the extravagancy of manufacturing those types of materials.

Furthermore, the mechanical analyses of reinforced concrete structures like plates can be established by using shear deformation plate theories. The non-local elasticity theory was firstly proposed by Eringen [22, 23]. The theory was subsequently developed by several researchers as a response to the inability of local elasticity so that to handle elastic problems with sharp geometrical singularities. For further reading, a synopsis of different non-local models can be found in Bažant and Jirásek [24]. Unlike its classical counterparts, the non-local theories contain internal material length scale parameters that can capture size effects at the nano scale Peddieson et al. [25], Sudak [26] and Amara et al. [27].

In view of the great practical importance of advanced composite materials, researchers like Bouiadjra et al. [28], Bessaim et al. [29], Yahia et al. [30], Attia et al. [31], have all presented various plate theories to investigate mechanical behaviors namely bending, buckling and vibration of functionally graded (FGM's) structures. Additionally, Mantari [32] presented a closed-form

solution of a generalized hybrid type quasi-3D high order shear deformation theory for the mechanical bending analysis of shells made of functionally graded material. Tounsi and his colleagues; Meziane et al. [33], and Beldjelili et al. [34], have developed a new refined and robust plate theory to analyze the free vibration of FGM as they proposed new refined plate theory with only four variables. Sayyad et al. [35] investigated the flexure of cross-ply laminated plates using an equivalent single layer trigonometric shear deformation theory while varying the mechanical bending loads. Mahjoobi and Bidgoli [36] proposes a mathematical model to analyze the dynamic response of a sandwich concrete plates attached with nano-fiber reinforced polymer (NFRP) layers, and subjected to blast loads. It considers the effects of parameters such as blast load, soil foundation, structural damping, and the volume fraction of carbon nano-fibers on the dynamic deflection of the structure. Results indicate that the NFRP layer improves the resistance of the concrete foundation against blast loads. Shamsavari et al. [37], on the other hand studied the free vibration of porous FG plates resting on Winkler/Pasternak/Kerr foundation using a novel Quasi-3D hyperbolic theory.

In this investigation, we aim to examine several variables influencing the bending performance of concrete slabs. These variables included the quantity of ferric oxide nanometric entities used as reinforcements, the geometric parameters of the plate, the effects of the surrounding soil medium, and the non-local parameters, focusing on identifying the optimal conditions for integrating these reinforcements into concrete matrices. By doing so, we aimed to unleash their full potential in improving the mechanical properties of the resulting composite material. To accomplish this, we adopt Eshelby's homogenization approach, which enables the determination of the elastic properties of the nano composites. Furthermore, we employ non-local Quasi-3D shear deformation theory to model the structure. Throughout our analysis, the concrete slab is subjected to various bending load patterns, with its support assumed to rest on the elastic foundation of Winkler-Pasternak-Kerr model. The primary objective of this study is to address the pressing issue of industrial iron waste, a notorious environmental pollutant, by exploring its potential utilization in concrete mixtures. Through recycling and integrating these waste materials into concrete formulations, we aim to assess and highlight their efficacy in enhancing the mechanical strength of the resultant concrete material.

2 Theory and formulations

In this section, analytical formulations are presented to simulate concrete plates impregnated with ferric oxide Fe_2O_3 nanoparticles, based on the kinematical and physical assumptions. Simply supported reinforced concrete plates are considered in this investigation, with dimensions: length a , width b and total thickness h .

The incorporated Fe_2O_3 nanoparticles are assumed to be randomly placed in the concrete matrix as illustrated in Fig. 1. The named coordinate system (x, y, z) is also shown in Fig. 1 at which Eq. (1):

$$0 \leq x < a; 0 \leq y < b; -h/2 \leq z < h/2. \quad (1)$$

2.1 Refined plate theory

In this analysis, we have incorporated various shear deformation theories for the purpose of comparison. Alongside the non-local quasi-3D shear deformation theory, we have also utilized the refined higher order deformation theory (RPT) proposed by Thai and Choi [38]. This comprehensive approach enables us to evaluate and compare the outcomes obtained from different theoretical perspectives. The RPT displacement field for a material point positioned at coordinates (x, y, z) within the plate can be expressed as follows in Eq. (2):

$$\begin{aligned} u_1(x, y, z) &= u_0(x, y) - z \frac{\partial w_b(x, t)}{\partial x} - f(z) \frac{\partial w_s(x, y)}{\partial x} \\ u_2(x, y, z) &= v_0(x, y) - z \frac{\partial w_b(x, t)}{\partial y} - f(z) \frac{\partial w_s(x, y)}{\partial y} \\ u_3(x, y, z) &= w_b(x, y) + w_s(x, y) \end{aligned} \quad (2)$$

$u_1, u_2,$ and u_3 are displacements within the x, y, z directions, u_0 and v_0 are displacements in mid-plane, w_b and w_s are the bending and shear components of the transverse displacement along z direction respectively. The $f(z)$ represents a shape function describing the distribution of the transverse shear strains and stresses along the thickness of the concrete slab [39] in Eq. (3).

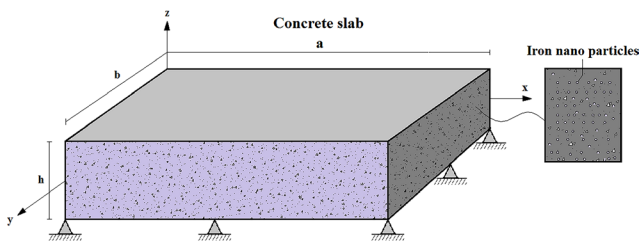


Fig. 1 Geometry and coordinate of a simply supported nano Fe_2O_3 -reinforced concrete

$$f(z) = z \left(\frac{1}{4} - \frac{5z^2}{3h^3} \right) \quad (3)$$

The displacement field of the classical plate theory (CLPT) can be obtained easily by considering $f(z) = 0$. The displacement of the first order shear deformation plate theory (FSDPT) can be obtained also by setting $f(z) = z$.

2.2 Refined Quasi-3D deformation plate theory

In the current formulation of the refined quasi-3D shear deformation plate theory, the displacement field is obtained on the basis of the following assumptions:

- The total transverse displacement u_3 in z direction is divided into 03 components, bending (w_b), shear (w_s), and thickness stretching effect (w_{st}). In this respect, the bending and shear components are functions of coordinates x and y only, and the stretching part is the functions x, y and z .
- The in-plane displacements (u_1 and u_2) in the coordinates x and y are considered to be divided into extension, bending and shear parts. It is shown that the in-plane displacements are functions of x, y and z in which the bending parts are alike to those presented by CPT, and shear parts of that are in relation with the hyperbolic variations of shear strains across the slab thickness.

Based on the above assumptions, the applicable displacement field can be defined as following in Eq. (4) [40]:

$$\begin{aligned} u_1(x, y, z) &= u_0(x, y) - z \frac{\partial w_b(x, t)}{\partial x} - f(z) \frac{\partial w_s(x, y)}{\partial x} \\ u_2(x, y, z) &= v_0(x, y) - z \frac{\partial w_b(x, t)}{\partial y} - f(z) \frac{\partial w_s(x, y)}{\partial y} \\ u_3(x, y, z) &= w_b(x, y) + w_s(x, y) + w_{st}(x, y). \end{aligned} \quad (4)$$

At this point, u_0 and v_0 signify the displacement functions of the mid surfaces of the plate. The $f(z)$ is the shape function that expresses the distribution of transverse shear stress across the plate thickness. In addition, the thickness stretching term can be expressed as Eq. (5):

$$w_{st}(x, y) = g(z) w_z(x, y) \quad (5)$$

where Eq. (6):

$$f(z) = z \left(\frac{1}{4} - \frac{5z^2}{3h^3} \right); g(z) = 1 - \frac{\partial f(z)}{\partial z}. \quad (6)$$

The linear strains associated with the Quasi-3D displacement equations can be denoted by Eq. (7):

$$\begin{aligned}
 \varepsilon_x &= \frac{\partial u_1}{\partial x} = \varepsilon_x^0 + zk_x^b + f(z)k_x^s; \\
 \varepsilon_y &= \frac{\partial u_2}{\partial y} = \varepsilon_y^0 + zk_y^b + f(z)k_y^s; \\
 \varepsilon_z &= \frac{\partial u_3}{\partial z} = \frac{\partial g(z)}{\partial z}w_z(x); \\
 \gamma_{xy} &= \frac{\partial u_1}{\partial y} + \frac{\partial u_2}{\partial x} = \gamma_{xy}^0 + z\gamma_{xy}^b + f(z)\gamma_{xy}^s; \\
 \gamma_{yz} &= \frac{\partial u_3}{\partial y} + \frac{\partial u_2}{\partial z} = \left(1 - \frac{\partial f(z)}{\partial z}\right)\gamma_{yz}^s = g(z)\gamma_{yz}^s; \\
 \gamma_{xz} &= \frac{\partial u_3}{\partial x} + \frac{\partial u_1}{\partial z} = \left(1 - \frac{\partial f(z)}{\partial z}\right)\gamma_{xz}^s = g(z)\gamma_{xz}^s;
 \end{aligned} \tag{7}$$

in which Eq. (8):

$$\begin{aligned}
 \varepsilon_x^0 &= \frac{\partial u_0}{\partial x}; k_x^b = -\frac{\partial^2 w_b}{\partial x^2}; k_x^s = -\frac{\partial^2 w_s}{\partial x^2}; \\
 \varepsilon_y^0 &= \frac{\partial v_0}{\partial y}; k_y^b = -\frac{\partial^2 w_b}{\partial y^2}; \\
 k_y^s &= -\frac{\partial^2 w_s}{\partial y^2}; \gamma_{xy}^0 = \frac{\partial u_0}{\partial y} + \frac{\partial v_0}{\partial x}; \\
 \gamma_{xy}^b &= -2\frac{\partial^2 w_b}{\partial x\partial y}; \gamma_{xy}^s = \frac{\partial^2 w_s}{\partial x\partial y}; \gamma_{xz}^s = \frac{\partial w_s}{\partial x}.
 \end{aligned} \tag{8}$$

2.3 Non-local elasticity theory

By taking into account the inter-molecular attractions of the composite material, the theory of non-local that considers the scale effect proposed by Eringen [22] indicates that the stresses at the reference point x in the material body depend not only on the deformations at x , but also on the deformations at all points of the body. Therefore, the constitutive stress-strain relations based of the non-local theory of the nano-composite can be defined as Eq. (9):

$$\begin{aligned}
 \begin{Bmatrix} \sigma_x \\ \sigma_y \\ \sigma_z \\ \tau_{xy} \\ \tau_{yz} \\ \tau_{xz} \end{Bmatrix} - \mu \nabla^2 \begin{Bmatrix} \sigma_x \\ \sigma_y \\ \sigma_z \\ \tau_{xy} \\ \tau_{yz} \\ \tau_{xz} \end{Bmatrix} &= \begin{bmatrix} C_{11}^T & C_{11}^T & C_{11}^T & 0 & 0 & 0 \\ C_{11}^T & C_{11}^T & C_{11}^T & 0 & 0 & 0 \\ C_{11}^T & C_{11}^T & C_{11}^T & 0 & 0 & 0 \\ 0 & 0 & 0 & C_{11}^T & 0 & 0 \\ 0 & 0 & 0 & 0 & C_{11}^T & 0 \\ 0 & 0 & 0 & 0 & 0 & C_{11}^T \end{bmatrix} \begin{Bmatrix} \varepsilon_x \\ \varepsilon_y \\ \varepsilon_z \\ \gamma_{xy} \\ \gamma_{yz} \\ \gamma_{xz} \end{Bmatrix}.
 \end{aligned} \tag{9}$$

At this juncture, C_{ij}^T tensor denotes the stiffness tensor of the reinforced concrete while $\mu = (e_0 a)^2$ is the non-local parameter, which depends on the appropriate material constant e_0 , whereas a represents the internal characteristic length. The term ∇^2 is the Laplace operator in (x, y) dimensional Cartesian coordinates. This latter term is expressed as Eq. (10):

$$\nabla^2 = \frac{d^2}{dx^2} + \frac{d^2}{dy^2}. \tag{10}$$

2.4 Homogenisation procedures

In order to assess the elastic properties of concrete reinforced with ferric oxide (Fe_2O_3), the application of Eshelby's homogenization model [41] appears to be more suitable. This model, primarily used for ellipsoidal inclusions in an infinite matrix [42], allows for the determination of equivalent properties of the plate. In the present study, the iron nanoparticles are assumed to be randomly distributed and possess a spherical shape. The stiffness tensor C^T for the reinforced plate can be expressed in matrix form as follows in Eq. (11):

$$C^T = \left(C_m^{-1} - V_r \left\{ (C_r - C_m) [S - V_r (S - I)] + C_m \right\}^{-1} \right)^{-1} \times (C_r - C_m) C_m^{-1} \tag{11}$$

In which, I is the identity matrix. C_m and C_r are the stiffness tensors for the concrete and ferric oxide (Fe_2O_3) reinforcements respectively. V_m and V_r are the volume fraction of the matrix and the reinforcement, while S is the Eshelby's tensor, which is in conjunction with the Poisson ratios of nanoparticles.

The stiffness tensors of iron nanoparticles C_r and of the concrete matrix C_m , which are considered isotropic, are expressed as Eq. (12):

$$\begin{aligned}
 C_\alpha^{11} &= C_\alpha^{22} = \frac{(1-\nu_\alpha)E_\alpha}{(1+\nu_\alpha)(1-2\nu_\alpha)}; \\
 C_\alpha^{12} &= \frac{\nu E_\alpha}{(1+\nu_\alpha)(1-2\nu_\alpha)}; \\
 C_\alpha^{66} &= C_\alpha^{55} = C_\alpha^{44} = \frac{E_\alpha}{(1+\nu_\alpha)}.
 \end{aligned} \tag{12}$$

Herein, E denotes the young's modulus either of the concrete matrix ($\alpha = m$), or the ferric oxide nanoparticle reinforcement ($\alpha = r$). The ν is the Poisson's ratio. The used indexes (1, 2, 3) stands for (x, y, z) directions of the Cartesian co-ordinate system of the plate respectively.

Eshelby's tensor S for reinforcement with spherical form, is given as Eq. (13):

$$S = \begin{bmatrix} S_{1111} & S_{1122} & S_{1133} & S_{1123} & S_{1113} & S_{1112} \\ S_{2211} & S_{2222} & S_{2233} & S_{2223} & S_{2213} & S_{2212} \\ S_{3311} & S_{3322} & S_{3333} & S_{3323} & S_{3313} & S_{3312} \\ S_{2311} & S_{2322} & S_{2333} & S_{2323} & S_{2313} & S_{2312} \\ S_{1311} & S_{1322} & S_{1333} & S_{1323} & S_{1313} & S_{1312} \\ S_{1211} & S_{1222} & S_{1233} & S_{1123} & S_{1213} & S_{1212} \end{bmatrix} \quad (13)$$

where Eq. (14):

$$S_{1111} = S_{2222} = S_{3333} = \frac{7 - 5\nu_r}{15(1 - \nu_r)}$$

$$S_{1122} = S_{1133} = S_{2233} = S_{2211} = S_{3311} = S_{3322} = \frac{-1 + 5\nu_r}{15(1 - \nu_r)} \quad (14)$$

$$S_{1212} = S_{1313} = S_{2323} = \frac{4 - 5\nu_r}{15(1 - \nu_r)}$$

The ν_r denotes here the Poisson's ratio of iron nanoparticles reinforcements.

2.5 Equations of motion

Next, the principle of the virtual work is applied in order to provide the equations of motion of the plate in Eq. (15):

$$\int_{t_1}^{t_2} (\delta U_p + \delta U_f + \delta V) \delta t = 0 \quad (15)$$

where δU_p and δU_f signify the virtual variation of the internal strain energy of the plate and the elastic foundation respectively. The δV is the virtual work that is done by external bending loads.

The expression of the virtual strain energy done by the plate is depicted as follows in Eq. (16):

$$\delta U_p = \int_0^L \int_{-h/2}^{h/2} \left(\sigma_x \delta \varepsilon_x + \sigma_y \delta \varepsilon_y + \sigma_z \delta \varepsilon_z + \tau_{xy} \delta \gamma_{xy} + \tau_{yz} \delta \gamma_{yz} + \tau_{xz} \delta \gamma_{xz} \right) dAdz \quad (16)$$

By substituting strain expression Eq. (7) in Eq. (16), one finds Eq. (17):

$$\delta U_b = \int_A \left(\begin{aligned} & N_x \frac{\partial \delta u_0}{\partial x} - M_x^b \frac{\partial^2 \delta w_b}{\partial^2 x} + M_x^s \frac{\partial^2 \delta w_s}{\partial^2 x} \\ & + N_y \frac{\partial \delta v_0}{\partial y} - M_y^b \frac{\partial^2 \delta w_b}{\partial^2 y} + M_y^s \frac{\partial^2 \delta w_s}{\partial^2 y} \\ & + N_{xy} \left(\frac{\partial \delta u_0}{\partial y} + \frac{\partial \delta v_0}{\partial x} \right) + 2M_x^b \frac{\partial^2 \delta w_b}{\partial x \partial y} \\ & + 2M_x^s \frac{\partial^2 \delta w_s}{\partial x \partial y} + Q_{yz} \left(\frac{\partial \delta w_s}{\partial y} + \frac{\partial \delta w_z}{\partial y} \right) \\ & + Q_{xz} \left(\frac{\partial \delta w_s}{\partial x} + \frac{\partial \delta w_z}{\partial x} \right) + R_z \delta w_z \end{aligned} \right) \quad (17)$$

Where the stress resultants generated by the internal strain energy can be defined as Eq. (18):

$$(N_x, N_y, N_{xy}) = \int_{-h/2}^{h/2} (\sigma_x, \sigma_y, \sigma_{xy}) dz;$$

$$(M_x^b, M_y^b, M_{xy}^b) = \int_{-h/2}^{h/2} z (\sigma_x, \sigma_y, \sigma_{xy}) dz;$$

$$(M_x^s, M_y^s, M_{xy}^s) = \int_{-h/2}^{h/2} f(z) (\sigma_x, \sigma_y, \sigma_{xy}) dz; \quad (18)$$

$$(Q_{xz}, Q_{yz}) = \int_{-h/2}^{h/2} g(z) (\tau_{xz}, \tau_{yz}) dz;$$

$$R_z = \int_{-h/2}^{h/2} \frac{dg(z)}{dz} w_z dz.$$

By substituting Eq. (9) into Eq. (18), one can obtain the stress resultants in the form of material stiffness and displacement components (u_0, v_0, w_b, w_s, w_z) in Eqs. (19)–(23):

$$\begin{Bmatrix} Q_{yz} \\ Q_{xz} \end{Bmatrix} = [A_{sij}] \begin{Bmatrix} \frac{\partial w_s}{\partial y} + \frac{\partial w_z}{\partial y} \\ \frac{\partial w_s}{\partial x} + \frac{\partial w_z}{\partial x} \end{Bmatrix} \quad (19)$$

$$\begin{Bmatrix} N_x \\ N_y \\ N_{xy} \end{Bmatrix} = [A_{ij}] \begin{Bmatrix} \frac{du_0}{dx} \\ \frac{dv_0}{dy} \\ \frac{du_0}{dy} + \frac{dv_0}{dx} \end{Bmatrix} - [B_{ij}] \begin{Bmatrix} \frac{d^2 w_b}{dx^2} \\ \frac{d^2 w_b}{dy^2} \\ -2 \frac{d^2 w_b}{dxdy} \end{Bmatrix} \quad (20)$$

$$- [B_{sij}] \begin{Bmatrix} \frac{d^2 w_s}{dx^2} \\ \frac{d^2 w_s}{dy^2} \\ -2 \frac{d^2 w_s}{dxdy} \end{Bmatrix} + \begin{Bmatrix} P_{13} w_z \\ P_{23} w_z \\ 0 \end{Bmatrix};$$

$$\begin{Bmatrix} M_x^b \\ M_y^b \\ M_{xy}^b \end{Bmatrix} = [B_{ij}] \begin{Bmatrix} \frac{du_0}{dx} \\ \frac{dv_0}{dy} \\ \frac{du_0}{dy} + \frac{dv_0}{dx} \end{Bmatrix} - [D_{ij}] \begin{Bmatrix} \frac{d^2 w_b}{dx^2} \\ \frac{d^2 w_b}{dy^2} \\ -2 \frac{d^2 w_b}{dxdy} \end{Bmatrix} \quad (21)$$

$$- [D_{sij}] \begin{Bmatrix} \frac{d^2 w_s}{dx^2} \\ \frac{d^2 w_s}{dy^2} \\ -2 \frac{d^2 w_s}{dxdy} \end{Bmatrix} + \begin{Bmatrix} S_{13} w_z \\ S_{23} w_z \\ 0 \end{Bmatrix};$$

$$\begin{Bmatrix} M_x^s \\ M_y^s \\ M_{xy}^s \end{Bmatrix} = [B_{sij}] \begin{Bmatrix} \frac{du_0}{dx} \\ \frac{dv_0}{dy} \\ \frac{du_0}{dy} + \frac{dv_0}{dx} \end{Bmatrix} - [D_{sij}] \begin{Bmatrix} \frac{d^2 w_b}{dx^2} \\ \frac{d^2 w_b}{dy^2} \\ -2 \frac{d^2 w_b}{dx dy} \end{Bmatrix} \quad (22)$$

$$- [H_{sij}] \begin{Bmatrix} \frac{d^2 w_s}{dx^2} \\ \frac{d^2 w_s}{dy^2} \\ -2 \frac{d^2 w_s}{dx dy} \end{Bmatrix} + \begin{Bmatrix} S_{s13} w_z \\ S_{s23} w_z \\ 0 \end{Bmatrix};$$

$$R_z = [P_{ij}] \begin{Bmatrix} \frac{du_0}{dx} \\ \frac{dv_0}{dy} \\ \frac{du_0}{dy} + \frac{dv_0}{dx} \end{Bmatrix} + [S_{ij}] \begin{Bmatrix} \frac{d^2 w_b}{dx^2} \\ \frac{d^2 w_b}{dy^2} \\ -2 \frac{d^2 w_b}{dx dy} \end{Bmatrix} \quad (23)$$

$$+ [S_{sij}] \begin{Bmatrix} \frac{d^2 w_s}{dx^2} \\ \frac{d^2 w_s}{dy^2} \\ -2 \frac{d^2 w_s}{dx dy} \end{Bmatrix} + L_{33} w_z$$

where Eq. (24):

$$\begin{aligned} & \{A_{ij}, B_{ij}, D_{ij}, B_{sij}, D_{sij}, H_{sij}\} \\ &= \int_{-h/2}^{h/2} \{1, z, z^2, f(z), zf(z), f(z)^2\} C_{ij} dz; \\ & \{A_{sij}\} = \int_{-h/2}^{h/2} \{g(z)^2\} C_{ij} dz; \\ & \{P_{ij}, S_{ij}, S_{sij}, L_{ij}\} = \int_{-h/2}^{h/2} \frac{dg(z)}{dz} \left\{1, z, f(z), \frac{dg(z)}{dz}\right\} C_{ij} dz. \end{aligned} \quad (24)$$

The strain energy generated by Winkler/Pasternak/Kerr elastic foundation can be expressed as Eq. (25):

$$\begin{aligned} \delta U_f &= - \int_A \int_{-h/2}^{h/2} \{U_{\text{Winkler}} + U_{\text{Pasternak}} + U_{\text{Kerr}}\} dz dA \\ &= -(q_{\text{Winkler}} + q_{\text{Pasternak}} + q_{\text{Kerr}}) \end{aligned} \quad (25)$$

In which the subscripts are denoting the type of elastic foundations. By substituting the expression of the distributed loads of each elastic foundation in Eq. (25), the expression of the virtual strain energy becomes Eq. (26):

$$\delta U_f = - \int_A \left(\left(K_w u_3 \delta u_3 - K_p \nabla^2 u_3 \delta u_3 \right) - \left(\frac{K_l K_u}{K_l + K_u} u_3 \delta u_3 - \frac{K_s K_u}{K_l + K_u} \nabla^2 u_3 \delta u_3 \right) \right) dA. \quad (26)$$

Where K_w and K_p are the transverse and shear stiffness coefficients of the Winkler-Pasternak foundation respectively. The Kerr model foundation contains three parameters counting a shear layer with stiffness K_s , independent upper and lower elastic layers modelled by distributed springs with the stiffness K_l and K_u respectively.

As for the reinforced concrete plates subjected to transverse bending loads q , the virtual work can be described as follows in Eq. (27):

$$\delta V = - \int_A q (\delta w_b + \delta w_s + g(z) \delta w_z) dA \quad (27)$$

by substituting the internal and the external strain energies expressed in Eqs. (17), (26) and (27) into Eq. (15), then, integrating by parts and collecting the coefficients of $\delta u_0, \delta v_0, \delta w_b, \delta w_s, \delta w_z$, the following equations of motion are obtained in Eq. (28):

$$\begin{aligned} \delta u_0 : \frac{\partial N_x}{\partial x} + \frac{\partial N_{xy}}{\partial y} &= 0; \\ \delta v_0 : \frac{\partial N_y}{\partial y} + \frac{\partial N_{xy}}{\partial x} &= 0; \\ \delta w_b : \left(\frac{\partial^2 M_x^b}{\partial x^2} - 2 \frac{\partial^2 M_{xy}^b}{\partial x \partial y} + \frac{\partial^2 M_y^b}{\partial y^2} \right) + q \\ &- \left(K_w (w_b + w_z + g w_z) - K_s \frac{\partial^2 (w_b + w_z + g w_z)}{\partial x^2} \right) = 0; \\ \delta w_s : \left(\frac{\partial^2 M_x^s}{\partial x^2} - 2 \frac{\partial^2 M_{xy}^s}{\partial x \partial y} + \frac{\partial^2 M_y^s}{\partial y^2} \right) + \left(\frac{\partial Q_{xz}}{\partial x} + \frac{\partial Q_{yz}}{\partial y} \right) + q \\ &- \left(K_w (w_b + w_z + g w_z) - K_s \frac{\partial^2 (w_b + w_z + g w_z)}{\partial x^2} \right) = 0; \\ \delta w_z : \left(\frac{\partial Q_{xz}}{\partial x} + \frac{\partial Q_{yz}}{\partial y} - R_z \right) + g(z) q &= 0. \end{aligned} \quad (28)$$

2.6 Navier's analytical solutions

Consider a simply supported rectangular concrete plate Fig. 2 with length a , width b and total thickness h under the transverse bending loads.

Based on Navier's solution approach, the admissible displacement functions in the form of trigonometric series which satisfy the boundary condition of the problems are illustrated below in Eq. (29):

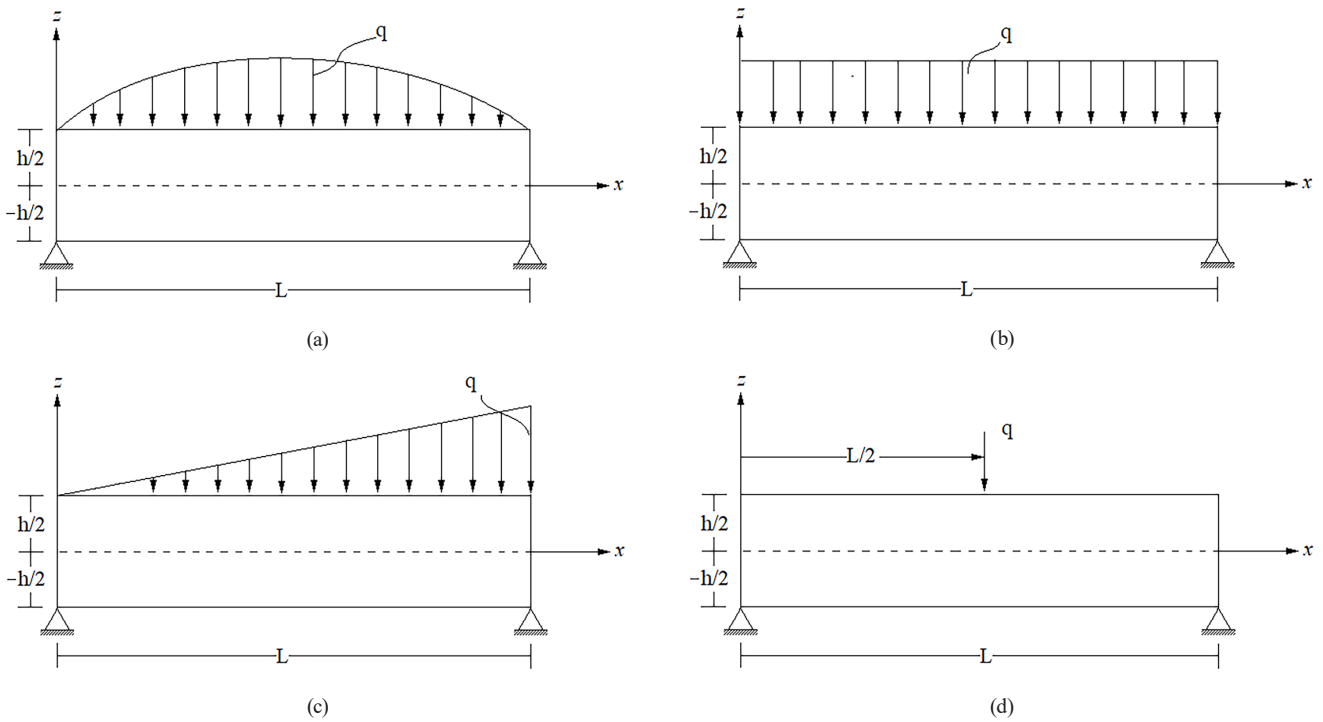


Fig. 2 Nano Fe₂O₃-reinforced concrete slabs resting on elastic foundation (a) under sinusoidal loading; and (b) under uniformly distributed loadings; (c) linearly distributed loading; and (d) concentrated loading

$$\begin{aligned}
 u_0(x, t) &= \sum_{n=1}^{\infty} U_{mn} \cos(\alpha x) \sin(\beta x); \\
 v_0(x, t) &= \sum_{n=1}^{\infty} V_{mn} \sin(\alpha x) \cos(\beta x); \\
 w_b(x, t) &= \sum_{n=1}^{\infty} W_{bmn} \sin(\alpha x) \sin(\beta x); \\
 w_s(x, t) &= \sum_{n=1}^{\infty} W_{smn} \sin(\alpha x) \sin(\beta x); \\
 w_z(x, t) &= \sum_{n=1}^{\infty} W_{zmn} \sin(\alpha x) \sin(\beta x);
 \end{aligned}
 \tag{29}$$

with $\alpha = m\pi/a$, $\beta = n\pi/b$, $(U_{mn}, V_{mn}, W_{bmn}, W_{smn}, W_{zmn})$ are the arbitrary parameters to be determined.

The proposed Navier's solution can satisfy the boundary conditions for a simply supported concrete plate in Eq. (30):

$$\begin{aligned}
 v_0(x, 0) &= \frac{dw_s(0, y)}{dy} = w_b(x, 0) = w_s(x, 0) = w_z(x, 0) \\
 &= N_x(x, 0) = M_x^b(x, 0) = M_x^s(x, 0) = 0; \\
 u_0(0, b) &= \frac{dw_s(0, b)}{dx} = w_b(0, b) = w_s(0, b) = w_z(0, b) \\
 &= N_y(0, b) = M_y^b(0, b) = M_y^s(0, b) = 0.
 \end{aligned}
 \tag{30}$$

The transverse bending load q can be also expanded in the Double-Fourier's sine series as Eq. (31):

$$q(x, y) = \sum_{m=1}^{\infty} \sum_{n=1}^{\infty} Q_{mn} \sin(\alpha x) \sin(\beta x) \tag{31}$$

where Eq. (32):

$$Q_{mn} = \begin{cases} q_0 & \text{for sinusoidal loading} \\ \frac{16q_0}{m\pi^2} & \text{for uniform load} \\ -\frac{8q_0}{m\pi^2} \cos(m\pi) & \text{for linear load} \\ \frac{4q_0}{ab} \sin\left(\frac{m\pi x_0}{a}\right) \sin\left(\frac{n\pi y_0}{b}\right) & \text{concentrated force.} \end{cases} \tag{32}$$

The closed-form solutions can be obtained from Eq. (33):

$$\begin{bmatrix} k_{11} & k_{12} & k_{13} & k_{14} & k_{15} \\ k_{21} & k_{22} & k_{23} & k_{24} & k_{25} \\ k_{31} & k_{32} & k_{33} & k_{34} & k_{35} \\ k_{41} & k_{42} & k_{43} & k_{44} & k_{45} \\ k_{51} & k_{52} & k_{53} & k_{54} & k_{55} \end{bmatrix} \begin{Bmatrix} U_{mn} \\ V_{mn} \\ W_{bmn} \\ W_{smn} \\ W_{zmn} \end{Bmatrix} = \begin{Bmatrix} 0 \\ 0 \\ Q_{mn} \\ Q_{mn} \\ Q_{mn} \end{Bmatrix} \tag{33}$$

where Eq. (34):

$$\begin{aligned}
 k_{11} &= -A_{11}\alpha^2 - A_{66}\beta^2; \quad k_{12} = -\alpha\beta(A_{66} + A_{12}); \\
 k_{13} &= B_{11}\alpha^3 + (2B_{66} + B_{12})\alpha\beta^2; \\
 k_{14} &= B_{s11}\alpha^3 + (2B_{s66} + B_{s12})\alpha\beta^2; \quad k_{15} = P_{13}\alpha; \\
 k_{21} &= k_{12}; \quad k_{22} = -(A_{11}\alpha^2 + A_{66}\beta^2); \quad k_{25} = P_{23}\beta; \\
 k_{23} &= B_{22}\beta^3 + (2B_{66} + B_{12})\alpha^2\beta; \\
 k_{24} &= B_{s22}\beta^3 + (2B_{s66} + B_{s12})\alpha^2\beta; \quad k_{31} = k_{13}; \\
 k_{32} &= k_{23}; \quad k_{33} = -D_{11}\alpha^4 - 2\alpha^2\beta^2(D_{12} + 2D_{66}) - D_{22}\beta^4; \\
 k_{34} &= -D_{s11}\alpha^4 - 2\alpha^2\beta^2(D_{s12} + 2D_{s66}) - D_{s22}\beta^4; \\
 k_{35} &= -S_{13}\alpha^2 - S_{23}\beta^2; \\
 k_{41} &= k_{14}; \quad k_{42} = k_{24}; \quad k_{43} = k_{34}; \\
 k_{44} &= -H_{s11}\alpha^4 - 2\alpha^2\beta^2(H_{s12} + 2H_{s66}) - H_{s22}\beta^4 \\
 &- A_{s55}\alpha^2 - A_{s44}\beta^2; \\
 k_{45} &= -A_{s44}\alpha^2 - A_{s55}\beta^2 - S_{s13}\alpha^2 - S_{s23}\beta^2; \quad k_{51} = k_{15}; \\
 k_{52} &= k_{25}; \quad k_{53} = k_{35}; \quad k_{54} = k_{45}; \\
 k_{55} &= -A_{s55}\alpha^2 - A_{s44}\beta^2 - L_{33}.
 \end{aligned} \tag{34}$$

3 Results and discussion

To evaluate the analytical bending behaviour of simply supported nano-Fe₂O₃ reinforced rectangular concrete slabs, a range of simulations are presented and discussed. It is important to emphasize that the objective of this research is to identify the most effective approach for utilizing iron nanoparticles in concrete matrices. Transverse displacements (\bar{w}), axial displacements (U), normal and shear stresses ($\bar{\sigma}_x, \bar{\tau}_{xz}$) are thus calculated using the refined Quasi-3D shear deformation theory.

In this analysis, the Young's modulus of the concrete slab is set to $E_m = 20$ GPa, the matrix is incorporated with ferric oxide Fe₂O₃ nanoparticles with Young's modulus of $E_r = 200$ GPa, and Poisson's ratios are $\nu_m = 0.3$ and $\nu_r = 0.291$ for concrete and iron nanoparticles respectively.

Dimensionless displacements and stresses engendered by the mechanical external loads are presented with reference to the following definitions in Eq. (35):

$$\begin{aligned}
 \bar{\sigma}_x(z) &= -\frac{h}{q_0L}\sigma_x\left(\frac{L}{2}, \frac{b}{2}, z\right); \\
 \bar{\sigma}_{xy}(z) &= \frac{h}{q_0L}\sigma_{xy}(0, 0, z); \\
 \bar{\tau}_{xz}(z) &= \frac{h}{q_0L}\tau_{xz}\left(0, \frac{b}{2}, z\right); \\
 \bar{w} &= \frac{10E_m h^3}{q_0L^4}w\left(\frac{L}{2}, \frac{b}{2}, z\right); \\
 U &= \frac{10E_m h^3}{q_0L^4}u\left(0, \frac{b}{2}, z\right).
 \end{aligned} \tag{35}$$

The non-dimensional coefficients of the three-parameter foundations are utilized as Eq. (36):

$$\begin{aligned}
 K_w &= \frac{k_w D_m}{L^4}; \quad K_p = \frac{k_p D_m}{L^2}; \quad K_l = \frac{k_l D_m}{L^4}; \\
 K_u &= \frac{k_u D_m}{L^4}; \quad K_s = \frac{k_s D_m}{L^2}; \quad D_m = \frac{E_m h^3}{12(1-\nu^2)}.
 \end{aligned} \tag{36}$$

3.1 Validation of the mathematical plate modelling

First, it is quite important to check the accuracy of the present mathematical model, since there are no numerical results in the literature regarding the bending analysis of iron nanoparticles reinforced concrete slabs.

By making allowance for the similar material and geometric parameters as proposed by Thai and Choi [40], and by eliminating the influence of iron nanoparticles and Winkler-Pasternak-Kerr foundation, the results of non-dimensional transverse displacements (\bar{w}) as well as shear stresses ($\bar{\tau}_{xz}$) of FG plates while varying the power index p are implemented to be compared with the present refined Quasi-3D theory.

The comparison of the results displayed in Table 1 [39, 40, 43, 44], elucidate that the different theories are in accordance with the predicted transverse displacement (\bar{w}) and shear stresses ($\bar{\tau}_{xz}$). Nevertheless, there is a slight difference in the current theory when compared to RPT and TSDT theories, as this is mainly because of the 3D-Quasi theory being used in our analysis, and which takes into account the stretching effect that evolves through the plate thickness. However, higher order shear deformation theories predict more accurate results than the first order (FSDT) and the classical (CPT) plate theories.

3.2 Validation of the homogenization model

Moreover, in order to validate the obtained elastic properties (reduced elastic constants C_{ij}^T) of a concrete matrix reinforced with iron oxide (Fe₂O₃) nanoparticles estimated using Eshelby's analytical approach and due to the lack of relevant studies dealing with similar analytical models, a comparison has been made between the elastic stiffness (C_{ij}^T) obtained from a concrete slab reinforced with iron nanoparticles (using the Eshelby's homogenization model), and the elastic stiffness (C_{ij}^T) obtained from a concrete slab reinforced with silica nanoparticles obtained by Chatbi et al. [9], using Voigt's homogenization model; without taking into account the agglomeration effects of SiO₂ nanoparticles in the matrix.

By way of explanation, Fig. 3 illustrates that both reinforcements (Fe₂O₃ and SiO₂) improved the elastic

Table 1 Comparison of the current plate theory to other published theories, ($a/h = 10, a = b$)

Theories	Shape function	$p = 0$		$p = 0.5$		$p = 1$		$p = 5$	
		\bar{w}	$\bar{\tau}_{xz}$	\bar{w}	$\bar{\tau}_{xz}$	\bar{w}	$\bar{\tau}_{xz}$	\bar{w}	$\bar{\tau}_{xz}$
Quasi-3D deformation theory: Thai and Choi [40]	$f(z) = z \left(1 - \frac{4z^2}{3h^2} \right)$	0.294	0.239	0.229	0.237	0.177	0.234	0.021	0.141
Refined plate theory (RPT): Thai and Choi [40]	$f(z) = z \left(\frac{1}{4} - \frac{5z^2}{3h^2} \right)$	0.296	0.239	0.231	0.237	0.181	0.234	0.025	0.141
Trigonometric shear deformation theory (TSDT): Reddy [39]	$f(z) = z \left(1 - \frac{4z^2}{3h^2} \right)$	0.296	0.239	0.231	0.237	0.181	0.234	0.025	0.141
First order shear deformation theory (FSDT): Whitney [43]*	$f(z) = z$	0.245	0.191	0.191	0.189	0.149	0.183	0.020	0.079
Classical plate theory (CPT): Kirchhoff [44]	$f(z) = 0$	0.280	–	0.219	–	0.171	–	0.024	–

* The shear correction factor for the FSDT is set to 5/6

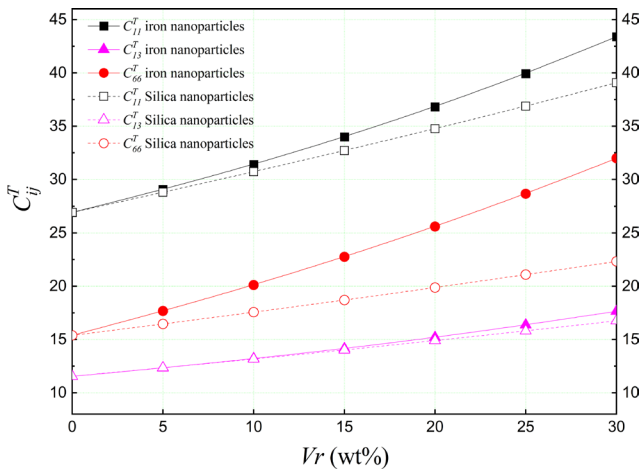


Fig. 3 A comparison between the obtained reduced elastic constants C_{ij}^T of nano-iron and nano-silica reinforced slabs

properties of the concrete, as it is also observed that the reduced elastic stiffness (C_{ij}^T) of the concrete slab grows up with an increasing reinforcement concentration (V_r). Yet, it is particularly detected in Fig. 3 that the stiffness of a concrete slab reinforced with iron nanoparticle (Fe_2O_3) is more improved than the nano scale silicon dioxide (SiO_2) reinforcement; especially in the case of (C_{13}^T) which represents the elastic stiffness in (x, z) plan of the plate. In this case, the stiffness tensor (C_{13}^T) increases by 40% for nano-silica reinforcement and almost doubles for iron oxide reinforcements. This improvement is mainly due to the high elastic properties of the iron nanoparticles.

3.3 Bending analysis of Fe_2O_3 reinforced concrete slab

In order to justify the choice of using iron nanoparticles in a concrete matrix as a reinforcement, the effect of Fe_2O_3 nanoparticles on the transverse displacement (\bar{w}) of a concrete plate is presented and compared to those of a concrete plate reinforced with SiO_2 silica nanoparticles (Fig. 4). The plate is simulated using the refined Quasi-3D

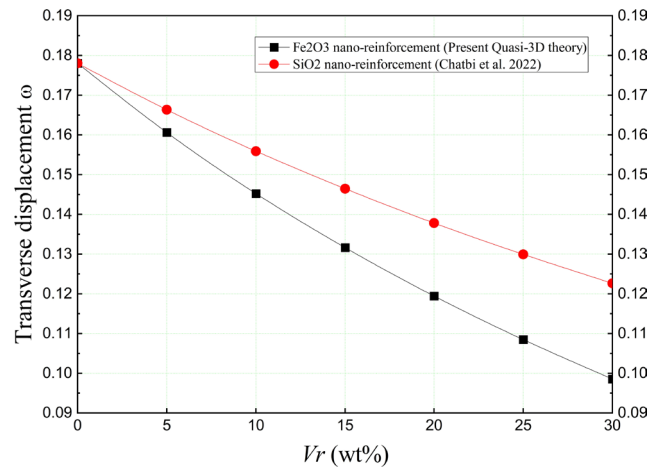


Fig. 4 A comparison between the effect of the using reinforcement nanoparticles on the transverse deflection of concrete slab ($a/h = 100$)

plate theory, while being considered as a simply supported and subjected to single-sine distributed loads.

As shown in Fig. 4, the non-dimensional transverse displacements (\bar{w}) are presented as a function of reinforcement volumes (V_r) that vary from 0% (unreinforced slab) to 30%. Apparently, for thin plates ($a/h = 100$), both reinforcements have a strengthening effect on the slab as the lateral displacement decreases by increasing the reinforcement volume in the concrete matrix. By incorporating 30 wt% of reinforcement, the lateral displacement tends to decrease by 30% for nano-silica reinforcement and 45% for ferric oxide nano-reinforcements.

However, the use of iron nanoparticles in the concrete matrix gives even more additional strength to the slab and makes it increasingly resistant to the external mechanical load.

Table 2 discloses the effect of thickness-to-length ratio on the non-dimensional transverse displacement, normal and shear stresses ($\bar{\sigma}_x, \bar{\tau}_{xz}$) of a simply supported reinforced concrete slab ($V_r = 20\%$) subjected to sinusoidal loading.

Table 2 Effect of thickness to length ration on the transvers displacement, normal and shear stress of a simply supported square plate subjected to sinusoidal load ($V_r = 20\%$)

Theories	Shape function	$L/h = 5$			$L/h = 10$			$L/h = 40$		
		\bar{w}	$\bar{\sigma}_x$	$\bar{\tau}_{xz}$	\bar{w}	$\bar{\sigma}_x$	$\bar{\tau}_{xz}$	\bar{w}	$\bar{\sigma}_x$	$\bar{\tau}_{xz}$
Quasi-3D deformation theory: Thai and Choi [40]	$f(z) = z \left(1 - \frac{4z^2}{3h^2} \right)$	0.1515	0.1384	0.1384	0.1511	0.1194	0.1515	0.1384	0.1384	0.1511
Refined plate theory (RPT): Thai and Choi [40]	$f(z) = z \left(\frac{1}{4} - \frac{5z^2}{3h^2} \right)$	0.1410	0.1573	0.1573	0.1532	0.1532	0.1410	0.1573	0.1573	0.1532
Trigonometric shear deformation theory (TSDT): Reddy [39]	$f(z) = z \left(1 - \frac{4z^2}{3h^2} \right)$	1.6963	1.5471	1.5471	1.9072	1.5072	1.6963	1.5471	1.5471	1.9072
First order shear deformation theory (FSDT): Whitney [43]*	$f(z) = z$	0.1400	0.1241	0.1241	0.1273	0.1194	0.1400	0.1241	0.1241	0.1273
Classical plate theory (CPT): Kirchhoff [44]	$f(z) = 0$	0.1343	0.1543	0.1543	0.1532	0.1532	0.1343	0.1543	0.1543	0.1532

* The shear correction factor for the FSDT is set to 5/6

The results related to the present refined Quasi-3D analytical are exhibited and thus compared with those estimated by the refined plate theory (RPT), the trigonometric plate theory (TPT), the first-order deformation theory (FSDT), and the classical plate theory (CPT). It is quite clear from the results listed in Table 2, that the trigonometric plate theory (TPT) is in a complete agreement with the refined theory of Thai and Choi [38], simply for the reason that both theories are HSDT's.

The remarkable difference between these two theories and the results of the present refined Quasi-3D theory is mainly due to the fact that the present theory takes into account the effect of the stretch that evolves through the plate thickness, making it therefore more accurate when compared to the other theories. However, the results obtained using CPT are rather less accurate.

Table 3 shows the effect of Fe_2O_3 reinforcement concentrations (V_r) in the concrete matrix on the non-dimensional lateral displacement (\bar{w}) of nanocomposite plate using the refined Quasi-3D plate theory. Several geometrical

ratios' (a/h) of a square plate (a/b) subjected to sinusoidal loads are considered. It can be inferred from the results in Table 3 that the lateral displacement decreases as the reinforcement volume in the concrete matrix increases with regard to the length-to-thickness ratio (a/h).

The effect of dissimilar external bending loads on the transverse displacement (\bar{w}) of a concrete plate reinforced with iron nanoparticles (Fe_2O_3) is represented in Fig. 5. The plate is simulated with the refined quasi-3D theory, whereas the displacements are calculated along the entire length of the plate (x/a). It is deduced from the results that the nanoparticles incorporated in the concrete matrix have a reinforcing effect regardless of the external applied mechanical load. Among the examined loads, the uniform load is the most critical one on the transverse displacement, while the concentrated load has the least effect on the plate. It is also worth noting that the maximum transverse displacement occurs at the mid-span of the plate for all types of loading.

The axial displacements (U) of nano-iron Fe_2O_3 reinforced concrete plate is illustrated in Fig. 6 in which several load patterns are considered. In this regard, we can observe that the axial displacements are symmetrical and they have the value 0 at the median plane ($z = 0$). This is mainly due to the accomplished homogeneity between the reinforcements and the matrix in the slabs using Eshelby's homogenisation approach besides the distribution assumptions of iron nanoparticles into the concrete matrix. We can also notice the difference between Fig. 6 (a) and Fig. 6 (b), in which the concentration of nano-iron plays a reinforcing role to reduce the axial displacements.

Table 3 The effect of the iron nanoparticles concentration V_r on the transverse deflection

a/h	Iron nano-particles volume V_r					
	0 wt%	5 wt%	10 wt%	15 wt%	20 wt%	30 wt%
4	0.2476	0.2207	0.1976	0.1775	0.1599	0.1305
10	0.2142	0.1917	0.1722	0.1551	0.1400	0.1305
20	0.2092	0.1874	0.1684	0.1518	0.1371	0.1123
40	0.2080	0.1863	0.1675	0.1510	0.1364	0.1117
70	0.2077	0.1861	0.1673	0.1508	0.1362	0.1116
100	0.2077	0.1860	0.1672	0.1507	0.1362	0.1116

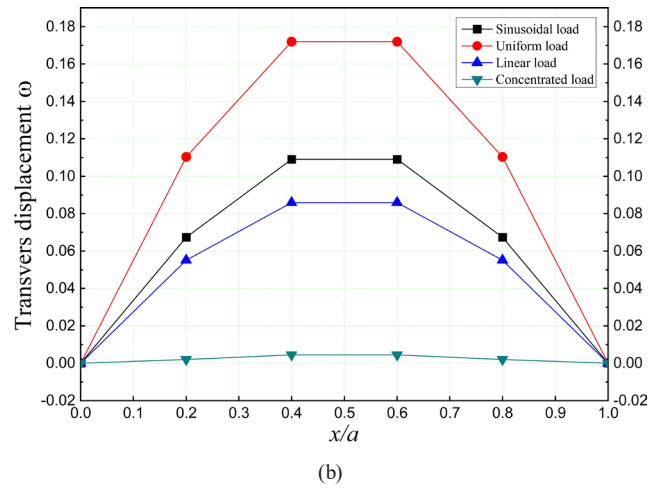
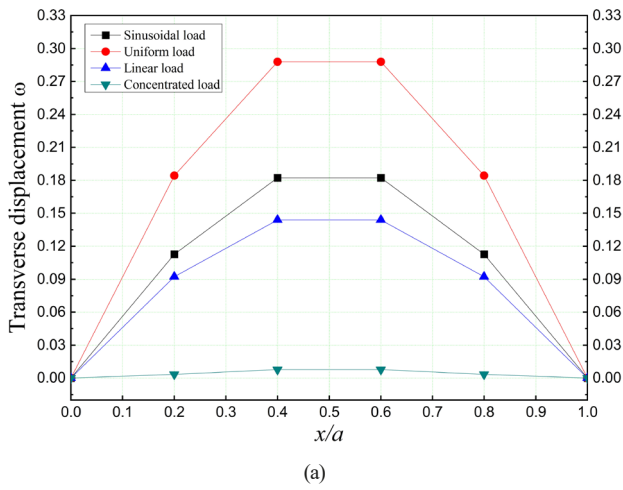


Fig. 5 The dimensionless transverse displacement of a RC slab under various types of loading, ($a/h = 4$): (a) $V_r = 5$ wt%; (b) $V_r = 30$ wt%

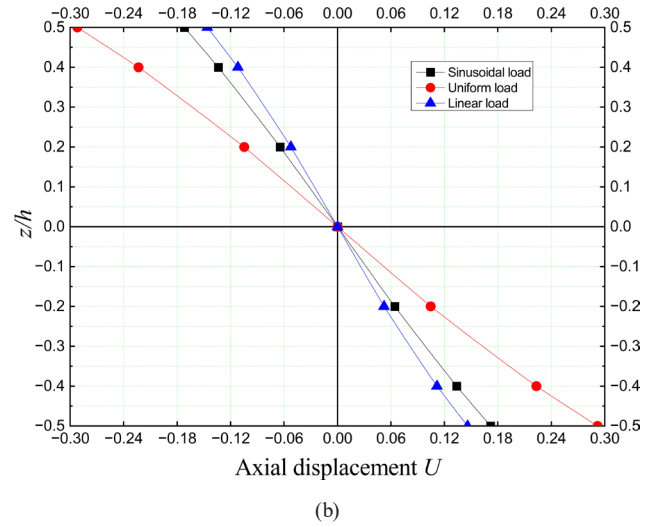
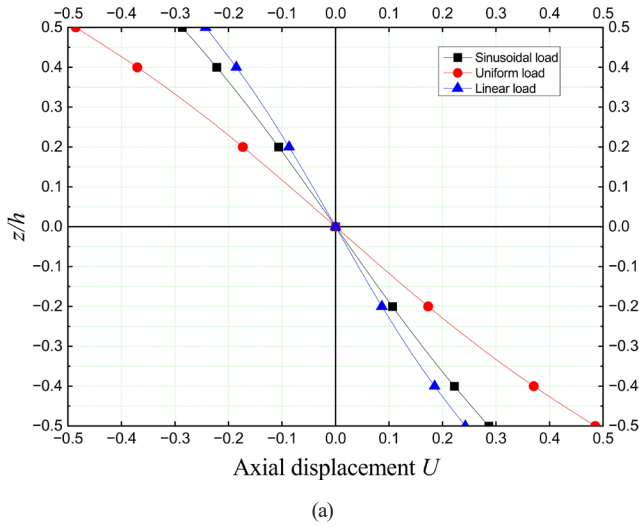


Fig. 6 The dimensionless axial displacement of a RC slab under various types of loading, ($a/h = 4$): (a) $V_r = 5$ wt%; (b) $V_r = 30$ wt%

By the application of different external bending loads on a nano-iron reinforced concrete plate, the non-dimensional shear stress ($\bar{\tau}_{xz}$) of a simply supported square plate

($a/b = 1$) is significantly presented in Fig. 7. As it has been observed before, the uniformly distributed load has the major effect on the shear stress of the reinforced plate, due

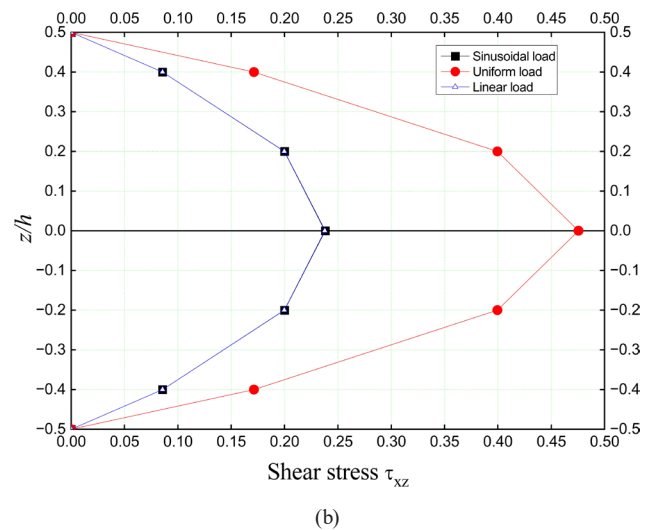
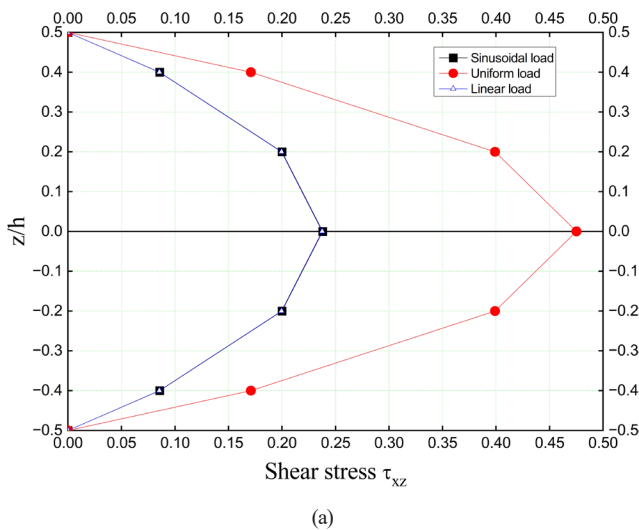


Fig. 7 The dimensionless shear stress of a RC slab under various types of loading, ($a/h = 4$): (a) $V_r = 5$ wt%; (b) $V_r = 30$ wt%

to the homogeneity of the nano composite plate in which we can see the symmetrical shape of stress distribution across the plate thickness (z/h). The symmetry is with respect to the mid-plane ($z = 0$), and it is where the stresses get their maximum values for all the loading cases.

3.4 Effect of Winkler/Pasternak elastic foundation on bending of Fe_2O_3 RC slabs

In order to widen the scope of this study, we will further assume that the ferric oxide (Fe_2O_3) reinforced concrete slab rests on an elastic foundation by introducing the elastic parameters. Fig. 8 embodies a concrete slab reinforced with Fe_2O_3 nanoparticles on a Winkler-Pasternak elastic foundation. This type of elastic foundation contains a shear layer of stiffness constant k_w , and a linked Pasternak springs of stiffness k_p .

Fig. 9 shows the effect of spring constant factors k_w and k_p on the transverse shear stress ($\bar{\tau}_{xz}$) of a square plate resting on Winkler-Pasternak's elastic foundation subjected to a sinusoidal bending loading. It can be detected that increasing the parameters of the elastic foundation leads to the decrease of the shear stress. One can also deduce that the maximum value emerges at the median plane of the plate and this is due to of the homogeneity of the nano-composite plate.

Fig. 9 shows the effect of spring constant factors k_w and k_p on the transverse shear stress ($\bar{\tau}_{xz}$) of a square plate resting on Winkler-Pasternak's elastic foundation subjected to a sinusoidal bending loading. It can be detected that

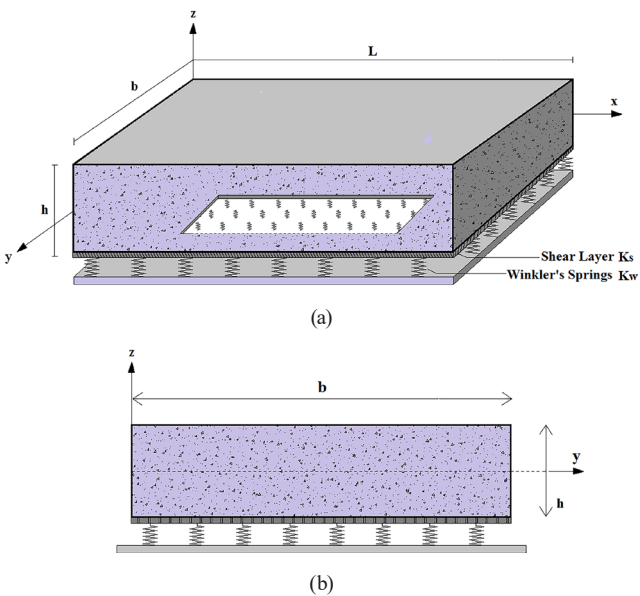


Fig. 8 A concrete slab reinforced with iron nanoparticles resting of elastic foundation (Winkler-Pasternak's type)

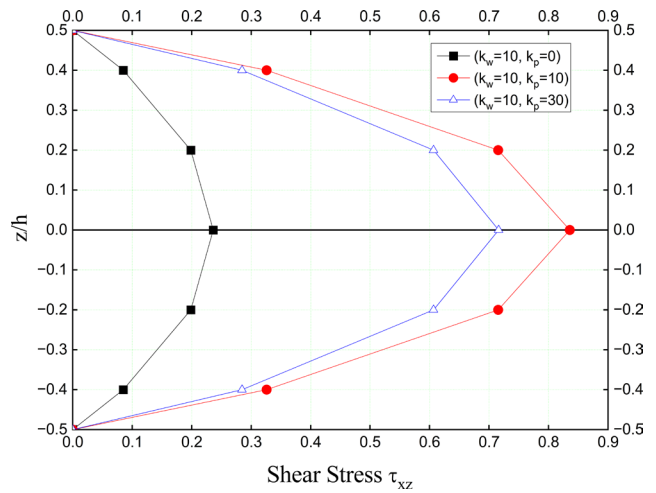


Fig. 9 The effect of the elastic foundation (Winkler-Pasternak model) on the shear stress of a reinforced concrete slab, ($a/h = 30, V_r = 30\%$)

increasing the parameters of the elastic foundation leads to the decrease of the shear stress. One can also deduce that the maximum value emerges at the median plane of the plate and this is due to of the homogeneity of the nano-composite plate.

As far as Fig. 10 is concerned, the refined Quasi-3D plate theory has been used in order to determine the effects of the shear layer constant k_p of Winkler-Pasternak's elastic foundation on the non-dimensional shear stress of ferric oxide reinforced concrete plate across the thickness of the plate (z/h).

It is thus obvious that the shear layer of Pasternak has a major effect on the non-dimensional shear stress of the plate, because the shear stress decreases as whilst the shear layer constant ks increases and this is noticeable along the entire thickness of the plate. It should be also noted that the effect of Pasternak's shear layer is rather more significant inside the plate.

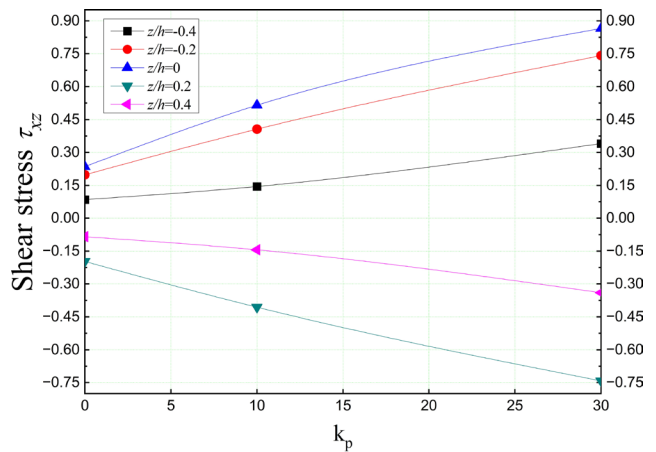


Fig. 10 The effect of the Pasternak's shear layer constant ks on the shear stress of a reinforced concrete plate, ($a/h = 4, V_r = 30\%, k_l = 0$)

3.5 Effect of Kerr elastic foundation on bending of Fe₂O₃ RC slabs

A simply supported square ($a/b = 1$) concrete plate on the top of Kerr's elastic foundation is illustrated in Fig. 11.

In order to analyze the effect of Kerr's elastic foundation on the dimensionless transverse displacement and the shear stresses of the nano composite plate, the refined Quasi-3D shear deformation theory is adopted, since this theory takes into account the stretching effect and the shear stress that evolve all over the slab thickness.

The results are hence presented in Table 4, as it worth pointing out that in order to reduce the computation rate, the Kerr's foundation's lower spring stiffness (k_l) is set to a constant value ($k_l = 10$).

It can be inferred from Table 4 that the shear layer ks and the upper spring parameters ku have a sliding effect on the dimensionless transverse displacement (\bar{w}) as well as on the transverse shear stress ($\bar{\tau}_{xz}$). In fact, the shear layer parameter (k_s) seems to be more effective than the upper

spring constant, with respect to the ferric oxide (Fe₂O₃) concentration exponent (V_r). It can be also deduced from Table 2 that the presence of an elastic Kerr foundation significantly affects the static response of the RC slab, causing therefore the deflection to decrease along increase of stiffness components.

3.6 Non-local bending analysis of Fe₂O₃ reinforced nano-slabs

Fig. 12 shows the effect of the non-local parameter (μ) on the non-dimensional deflection (\bar{w}) of a simply supported nano-iron reinforced concrete nano plate. The nano-sized plate is deemed to be subjected to a sinusoidal distributed bending load. The calculated values using the non-local refined Quasi-3D plate theory are compared to those estimated by other plate theories. In this respect, a wide range of non-local parameters (μ) are used, while the reinforcement volume concentration (V_r) is set to 15% and the length/depth ratio ($a/h = 10$).

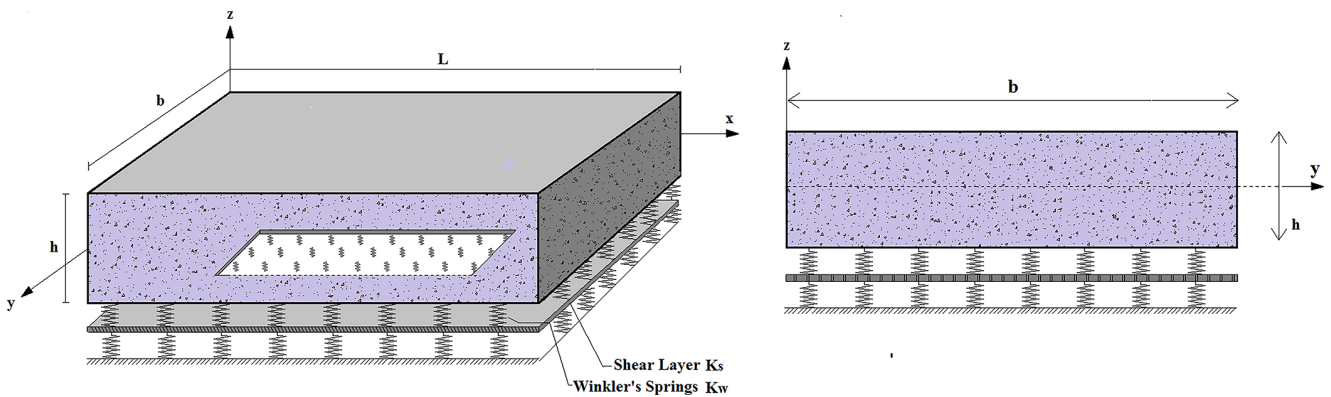


Fig. 11 A concrete slab reinforced with iron nanoparticles resting of Kerr's elastic foundation

Table 4 The non-dimensional transverse deflection and shear stresses of a S-S iron nanoparticles RC slab resting on Kerr elastic foundation ($k_l = 10, a = b$)

a/h	$(k_u; k_s)$	$\bar{w} (\times 10)$					
		$V_r = 5\%$	$V_r = 15\%$	$V_r = 30\%$	$V_r = 5\%$	$V_r = 15\%$	$V_r = 30\%$
4	(10;0)	2.2068	1.7748	1.3047	0.2381	0.2381	0.2381
10		1.1265	0.9116	0.6739	0.2386	0.2386	0.2386
20		0.5791	0.4691	0.3471	0.2387	0.2387	0.2387
100		0.1168	0.0946	0.07	0.2387	0.2387	0.2387
4	(10;10)	1.7109	2.3321	4.2036	0.3179	0.3771	0.4847
10		0.4957	0.5507	0.6964	0.6023	0.6427	0.7496
20		0.102	0.1063	0.1154	0.5235	0.5355	0.5609
100		0.00358	0.00361	0.00366	0.4849	0.4867	0.4901
4	(10;20)	1.7542	2.0935	3.4403	0.8412	0.958	1.4213
10		0.2031	0.2115	0.2296	0.5367	0.549	0.5756
20		0.0469	0.0477	0.0495	0.5004	0.5053	0.515
100		0.00176	0.00177	0.00178	0.4812	0.4821	0.4837

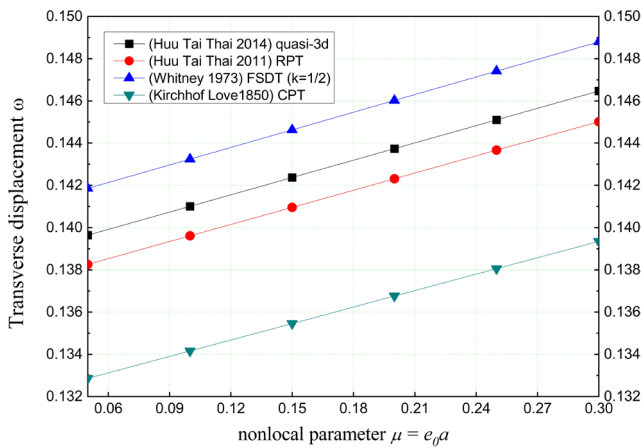


Fig. 12 The effect of the non-local parameter on the transverse displacement of RC plates, ($a/h = 10, V_f = 15\%$)

In view of Thai and Choi [38] mathematical formulation of the refined plate theory (RPT), the first order shear deformation theory and the classical plate theory (CPT) while considering the effect of Eringen's non-local theory, it is thus observed that the refined Quasi-3D and the RPT theories are in agreement, except for a slight difference between them due to the stretching effect that is evident in the Quasi-3D theory. Another exception concerns the classical plate theory (CPT) that neglects the shear effect in thick plates. However, in all plate theories, increasing the non-local parameter leads to an increase in deflections.

At last, Table 5 represents the effect of the non-local parameter (μ) on the non-dimensional deflection (\bar{w}), normal and shear stresses ($\bar{\sigma}_x, \bar{\tau}_{xz}$), while several proportions of reinforcement concentrations in the concrete plate are taken into consideration. It should be noted that $\mu = 0$; corresponds to the local plate theory. In regard of to the size

Table 5 The dimensionless transverse deflection (\bar{w}), normal stress ($\bar{\sigma}_x$), and shear stress ($\bar{\tau}_{xz}$) of nano-slabs reinforced with iron nanoparticles

a/h	$\mu = 0$			$\mu = 0.1$		
	\bar{w}	$\bar{\sigma}_x$	$\bar{\tau}_{xz}$	\bar{w}	$\bar{\sigma}_x$	$\bar{\tau}_{xz}$
4	0.2532	0.1668	0.2460	0.2782	0.1813	0.2674
10	0.2019	0.1577	0.2461	0.2219	0.1714	0.2675
20	0.1634	0.1511	0.2461	0.1796	0.1642	0.2675
100	0.1334	0.1465	0.2461	0.1466	0.1592	0.2675
a/h	$\mu = 0.2$			$\mu = 0.3$		
	\bar{w}	$\bar{\sigma}_x$	$\bar{\tau}_{xz}$	\bar{w}	$\bar{\sigma}_x$	$\bar{\tau}_{xz}$
4	0.3087	0.2012	0.2968	0.3393	0.2211	0.3262
10	0.2463	0.1902	0.2968	0.2707	0.2090	0.3262
20	0.1993	0.1823	0.2969	0.2191	0.2003	0.3263
100	0.1627	0.1766	0.2969	0.1788	0.1941	0.3263

of the plate, the iron volumes have the same strengthening effect on the matrix. It decreases the transverse displacement making therefore the plate less bent.

4 Conclusions

An analytical model has been proposed for simulating a concrete plate reinforced with iron nanoparticles. To enhance the comprehension of the static behaviour of nano-iron reinforced concrete slabs, a refined Quasi-3D slab theory, accounting for the stretching effect, was meticulously incorporated for analysis and achieving research objectives. Various types of loads were applied to the slab, under the assumption of it resting on an elastic Winkler-Pasternak-Kerr foundation. Finally, Eringen's non-local theory was employed to precisely characterize the static behaviour of the slab at the nano-scale level.

The following succinctly summarizes the research paper's main conclusions:

- Incorporating iron nanoparticles Fe_2O_3 in a concrete matrix improves the elastic properties of the mixture.
- Fe_2O_3 nanoparticles makes the reinforced concrete plates more resilient to the external mechanical bending loads.
- Increasing the concentrations of iron nanoparticles in the matrix significantly reduces the transverse deflection of concrete plates subjected to concentrated, single sine, uniformly, and linearly distributed loads.
- The presence of Winkler-Pasternak-Kerr elastic foundations significantly reduces the transverse displacement and shear stress of the reinforced concrete plate.
- As far as the size of the plate is concerned (macro or nano-sized plate), the iron volumes have the same reinforcing effect on the matrix. It decreases the transverse displacement, which makes the plate less curved.

Finally, the researchers anticipate that the findings from this study will provide preliminary insights into predicting the mechanical behavior and elastic properties of nanoparticle-reinforced concretes. This predictive capability will allow for informed assessments of the effects of these nanoparticles, thereby enabling researchers to anticipate outcomes before conducting expensive experiments.

Acknowledgement

The Thematic Agency for Research in Science and Technology (ATRST) of Algiers, Algeria is gratefully acknowledged.

References

- [1] Gopalakrishnan, K., Birgisson, B., Taylor, P., Attoh-Okine, N. O. "Nanotechnology in civil infrastructure: a paradigm shift", Springer, 2011. ISBN 978-3-642-16656-3
<https://doi.org/10.1007/978-3-642-16657-0>
- [2] Chatbi, M., Harrat, Z. R., Benatta, M. A., Krour, B., Hadzima-Nyarko, M., Işık, E., Czarnecki, S., Bouiadjra, M. B. "Nano-Clay Platelet Integration for Enhanced Bending Performance of Concrete Beams Resting on Elastic Foundation: An Analytical Investigation", *Materials*, 16(14), 5040, 2023.
<https://doi.org/10.3390/ma16145040>
- [3] Priyadarshana, T., Dissanayake, R. "Chloride Penetration and Sulfate Resistance of Concrete Incorporating Nano-Silica (Nano-SiO₂) Micro-Silica (Micro-SiO₂) and Fly Ash", In: *Proceedings of Fourth International Conference on Advances in Civil, Structural and Mechanical Engineering - ACSM 2016*, Institute of Research Engineers and Doctors, 2016, pp. 28–32. ISBN 978-1-63248-096-5
<https://doi.org/10.15224/978-1-63248-096-5-14>
- [4] Mondal, P., Shah, S. P., Marks, L. D., Gaitero, J. J. "Comparative Study of the Effects of Microsilica and Nanosilica in Concrete", *Journal of the Transportation Research Record*, 2141(1), pp. 6–9, 2010.
<https://doi.org/10.3141/2141-02>
- [5] Rong, Z., Sun, W., Xiao, H., Jiang, G. "Effects of Nano-SiO₂ Particles on the Mechanical and Microstructural Properties of Ultra-High Performance Cementitious Composites", *Cement and Concrete Composites*, 56, pp. 25–31, 2015.
<https://doi.org/10.1016/j.cemconcomp.2014.11.001>
- [6] Behzadian, R., Shahrajabian, H. "Experimental Study of the Effect of Nano-Silica on the Mechanical Properties of Concrete/PET Composites", *KSCE Journal of Civil Engineering*, 23(8), pp. 3660–3668, 2019.
<https://doi.org/10.1007/s12205-019-2440-9>
- [7] Bidgoli, M. R., Saedifar, M. "Time-dependent buckling analysis of SiO₂ nanoparticles reinforced concrete columns exposed to fire", *Computers and Concrete*, 20(2), pp. 119–127, 2017.
<https://doi.org/10.12989/cac.2017.20.2.119>
- [8] Harrat, Z. R., Amziane, S., Krour, B., Bouiadjra, M. B. "On the Static Behavior of Nano SiO₂ Based Concrete Beams Resting on an Elastic Foundation", *Computers and Concrete*, 27(6), pp. 575–583, 2021.
<https://doi.org/10.12989/cac.2021.27.6.575>
- [9] Chatbi, M., Krour, B., Benatta, M. A., Harrat, Z. R., Amziane, S., Bouiadjra, M. B. "Bending Analysis of Nano-SiO₂ Reinforced Concrete Slabs Resting on Elastic Foundation", *Structural Engineering and Mechanics*, 84(5), pp. 685–697, 2022.
<https://doi.org/10.12989/SEM.2022.84.5.685>
- [10] Jassas, M. R., Bidgoli, M. R., Kolahchi, R. "Forced Vibration Analysis of Concrete Slabs Reinforced by Agglomerated SiO₂ Nanoparticles Based on Numerical Methods", *Construction and Building Materials*, 211, pp. 796–806, 2019.
<https://doi.org/10.1016/j.conbuildmat.2019.03.263>
- [11] Rashmi, R., Padmapriya, R. "Experimental and Analytical Study on Flexural Behavior of Reinforced Concrete Beams Using Nano Silica", *Materials Today: Proceedings*, 50, pp. 57–69, 2022.
<https://doi.org/10.1016/j.matpr.2021.04.127>
- [12] Nazari, A., Riahi, S. "The Effects of ZrO₂ Nanoparticles on Physical and Mechanical Properties of High Strength Self Compacting Concrete", *Materials Research*, 13(4), pp. 551–556, 2010.
<https://doi.org/10.1590/S1516-14392010000400019>
- [13] Aly, M., Hashmi, M. S. J., Olabi, A. G., Messeiry, M., Hussain, A. I. "Effect of Nano Clay Particles on Mechanical, Thermal and Physical Behaviours of Waste-Glass Cement Mortars", *Materials Science and Engineering: A*, 528(27), pp. 7991–7998, 2011.
<https://doi.org/10.1016/j.msea.2011.07.058>
- [14] Guo, M.-Z., Ling, T.-C., Poon, C.-S. "Nano-TiO₂-based Architectural Mortar for NO Removal and Bacteria Inactivation: Influence of Coating and Weathering Conditions", *Cement and Concrete Composites*, 36, pp. 101–108, 2013.
<https://doi.org/10.1016/j.cemconcomp.2012.08.006>
- [15] Feng, D., Xie, N., Gong, C., Leng, Z., Xiao, H., Li, H., Shi, X. "Portland Cement Paste Modified by TiO₂ Nanoparticles: A Microstructure Perspective", *Industrial & Engineering Chemistry Research*, 52(33), pp. 11575–11582, 2013.
<https://doi.org/10.1021/ie4011595>
- [16] Joshaghani, A., Balapour, M., Mashhadian, M., Ozbakkaloglu, T. "Effects of Nano-TiO₂, Nano-Al₂O₃, and Nano-Fe₂O₃ on Rheology, Mechanical and Durability Properties of Self-Consolidating Concrete (SCC): An Experimental Study", *Construction and Building Materials*, 245, 118444, 2020.
<https://doi.org/10.1016/j.conbuildmat.2020.118444>
- [17] Amoli, A., Kolahchi, R., Bidgoli, M. R. "Seismic Analysis of Al₂O₃ nanoparticles-reinforced concrete plates based on sinusoidal shear deformation theory", *Earthquakes and Structures*, 15(3), pp. 285–294, 2018.
<https://doi.org/10.12989/eas.2018.15.3.285>
- [18] Nazari, A., Riahi, S., Riahi, S., Shamekhi, S. F., Khademno, A. "Benefits of Fe₂O₃ Nanoparticles in Concrete Mixing Matrix", *Journal of American Science*, 6(4), pp. 102–106, 2010.
- [19] Nazari, A., Riahi, S., Riahi, S., Shamekhi, S. F., Khademno, A. "The Effects of Incorporation Fe₂O₃ Nanoparticles on Tensile and Flexural Strength of Concrete", *Journal of American Science*, 6(4), pp. 90–93, 2010.
- [20] Salemi, N., Behfarnia, K., Zaree, S. A. "Effect of Nanoparticles on Frost Durability of Concrete", *Asian Journal of Civil Engineering*, 15(3), pp. 411–420, 2014.
- [21] Nouri, A. Z. "The Effect of Fe₂O₃ Nanoparticles Instead Cement on the Stability of Fluid-Conveying Concrete Pipes Based on Exact Solution", *Computers and Concrete*, 21(1), pp. 31–37, 2018.
<https://doi.org/10.12989/cac.2018.21.1.031>
- [22] Eringen, A. C. "On Differential Equations of Nonlocal Elasticity and Solutions of Screw Dislocation and Surface Waves", *Journal of Applied Physics*, 54(9), pp. 4703–4710, 1983.
<https://doi.org/10.1063/1.332803>
- [23] Eringen, A. C. "Nonlocal Polar Elastic Continua", *International Journal of Engineering Science*, 10(1), pp. 1–16, 1972.
[https://doi.org/10.1016/0020-7225\(72\)90070-5](https://doi.org/10.1016/0020-7225(72)90070-5)
- [24] Bažant, Z. P., Jirásek, M. "Nonlocal Integral Formulations of Plasticity and Damage: Survey of Progress", *Journal of Engineering Mechanics*, 128(11), pp. 1119–1149, 2002.
[https://doi.org/10.1061/\(ASCE\)0733-9399\(2002\)128:11\(1119\)](https://doi.org/10.1061/(ASCE)0733-9399(2002)128:11(1119))

- [25] Peddieson, J., Buchanan, G. R., McNitt, R. P. "Application of non-local continuum models to nanotechnology", *International Journal of Engineering Science*, 41(3–5), pp. 305–312, 2003.
[https://doi.org/10.1016/S0020-7225\(02\)00210-0](https://doi.org/10.1016/S0020-7225(02)00210-0)
- [26] Sudak, L. J. "Column Buckling of Multiwalled Carbon Nanotubes Using Nonlocal Continuum Mechanics", *Journal of Applied Physics*, 94(11), pp. 7281–7287, 2003.
<https://doi.org/10.1063/1.1625437>
- [27] Amara, K., Tounsi, A., Mechab, I., Adda-Bedia, E. A. "Nonlocal elasticity effect on column buckling of multiwalled carbon nanotubes under temperature field", *Applied Mathematical Modelling*, 34(12), pp. 3933–3942, 2010.
<https://doi.org/10.1016/j.apm.2010.03.029>
- [28] Bouiadjra, M. B., Ahmed Houari, M. S., Tounsi, A. "Thermal Buckling of Functionally Graded Plates According to a Four-Variable Refined Plate Theory", *Journal of Thermal Stresses*, 35(8), pp. 677–694, 2012.
<https://doi.org/10.1080/01495739.2012.688665>
- [29] Bessaim, A., Houari, M. S. A., Tounsi, A., Mahmoud, S. R., Bedia, E. A. A. "A new higher-order shear and normal deformation theory for the static and free vibration analysis of sandwich plates with functionally graded isotropic face sheets", *Journal of Sandwich Structures & Materials*, 15(6), pp. 671–703, 2013.
<https://doi.org/10.1177/1099636213498888>
- [30] Yahia, S. A., Atmane, H. A., Houari, M. S. A., Tounsi, A. "Wave propagation in functionally graded plates with porosities using various higher-order shear deformation plate theories", *Structural Engineering and Mechanics*, 53(6), pp. 1143–1165, 2015.
<https://doi.org/10.12989/sem.2015.53.6.1143>
- [31] Attia, A., Bousahla, A. A., Tounsi, A., Mahmoud, S. R., Alwabri, A. S. "A refined four variable plate theory for thermoelastic analysis of FGM plates resting on variable elastic foundations", *Structural Engineering and Mechanics*, 65(4), pp. 453–464, 2018.
<https://doi.org/10.12989/sem.2018.65.4.453>
- [32] Mantari, J. L. "Refined and generalized hybrid type quasi-3D shear deformation theory for the bending analysis of functionally graded shells", *Composites Part B: Engineering*, 83, pp. 142–152, 2015.
<https://doi.org/10.1016/j.compositesb.2015.08.048>
- [33] Meziane, M. A. A., Abdelaziz, H. H., Tounsi, A. "An efficient and simple refined theory for buckling and free vibration of exponentially graded sandwich plates under various boundary conditions", *Journal of Sandwich Structures & Materials*, 16(3), pp. 293–318, 2014.
<https://doi.org/10.1177/1099636214526852>
- [34] Beldjelili Y, Tounsi, A., Mahmoud, S. R. "Hygro-thermo-mechanical bending of S-FGM plates resting on variable elastic foundations using a four-variable trigonometric plate theory", *Smart Structures and Systems*, 18(4), pp. 755–786, 2016.
<https://doi.org/10.12989/sss.2016.18.4.755>
- [35] Sayyad, A. S. Ghugal, Y. M. "Flexure of cross-ply laminated plates using equivalent single layer trigonometric shear deformation theory", *Structural Engineering and Mechanics*, 51(5), pp. 867–891, 2014.
<https://doi.org/10.12989/sem.2014.51.5.867>
- [36] Mahjoobi, M., Bidgoli, M. R. "Dynamic deflection analysis induced by blast load in viscoelastic sandwich plates with nanocomposite facesheets", *Journal of Sandwich Structures & Materials*, 23(4), pp. 1118–1140, 2021.
<https://doi.org/10.1177/1099636219853189>
- [37] Shahsavari, D., Karami, B., Fakhham, H. R., Li, L. "On the shear buckling of porous nanoplates using a new size-dependent quasi-3D shear deformation theory", *Acta Mechanica*, 229(11), pp. 4549–4573, 2018.
<https://doi.org/10.1007/s00707-018-2247-7>
- [38] Thai, H.-T., Choi, D.-H. "A refined plate theory for functionally graded plates resting on elastic foundation", *Composites Science and Technology*, 71(16), pp. 1850–1858, 2011.
<https://doi.org/10.1016/j.compscitech.2011.08.016>
- [39] Reddy, J. N. "A general non-linear third-order theory of plates with moderate thickness", *International Journal of Non-Linear Mechanics*, 25(6), pp. 677–686, 1990.
[https://doi.org/10.1016/0020-7462\(90\)90006-U](https://doi.org/10.1016/0020-7462(90)90006-U)
- [40] Thai, H.-T., Choi, D.-H. "Improved refined plate theory accounting for effect of thickness stretching in functionally graded plates", *Composites Part B: Engineering*, 56, pp. 705–716, 2014.
<https://doi.org/10.1016/j.compositesb.2013.09.008>
- [41] Eshelby, J. D. "The determination of the elastic field of an ellipsoidal inclusion, and related problems", *Proceedings of the Royal Society of London Series A: Mathematical and Physical Sciences*, 241(1226), pp. 376–396, 1957.
<https://doi.org/10.1098/rspa.1957.0133>
- [42] Clyne, T. W., Withers, P. J. "An Introduction to Metal Matrix Composites", [e-book], Cambridge University Press, 1993. ISBN 9780511623080
<https://doi.org/10.1017/CBO9780511623080>
- [43] Whitney, J. M. "Shear Correction Factors for Orthotropic Laminates under Static Load", *Journal of Applied Mechanics*, 40(1), pp. 302–304, 1973.
<https://doi.org/10.1115/1.3422950>
- [44] Kirchhoff, G. "Über das Gleichgewicht und die Bewegung einer elastischen Scheibe" (In regards to the equilibrium and motion of an elastic disk), *Journal für die reine und angewandte Mathematik (Crelles Journal)*, 1850(40), pp. 51–88, 1850. (in German)
<https://doi.org/10.1515/crll.1850.40.51>